PROCEEDINGS, 48th Workshop on Geothermal Reservoir Engineering
Stanford University, Stanford, California, February 6-8, 2023
SGP-TR-224

Stability and Breakdown of Acid-Induced Hydrated Silicate Gels and Metal Silicates under Geothermal Conditions: A Preliminary Laboratory Study

Seiji Nakagawa[1], William Kibikas[2], Chun Chang[1], Timothy Kneafsey[1], Patrick Dobson[1], Abraham Samuel[3] Michael Otto[4], Stephen Bruce[4], Nils Kaargeson-Loe[4], Stephen J. Bauer[2]

[1]Lawrence Berkeley National Laboratory, Berkeley, CA 94720, [2]Sandia National Laboratories, Albuquerque, NM 87185, [3]Geothermal Resource Group Inc., Palm Desert, California, USA, [4]Baker Hughes Inc., Houston, Texas, USA

snakagawa@lbl.gov[1], chunchang@lbl.gov[1], wmkibiks@sandia.gov[2], tjkneafsey@lbl.gov[1], pfdobson@lbl.gov[1], samabraham@geothermalresourcegroup.com[3], Michael.Otto@bakerhughes.com[4], stephen.bruce@bakerhughes.com[4], Nils.Kaageson-Loe@bakerhughes.com[4], sjbauer001@gmail.com[2]

Keywords: flow diverter; silicate gel; metal silicate; gel stability; laboratory experiment

ABSTRACT

We conducted a series of laboratory experiments by mixing sodium silicate with different concentrations of 1) acid (for acid-induced hydrated silicate gel) or 2) metal chloride or acetate (for metal-silicate). Stability of the produced gels and precipitates was tested after heating at 200 ˚C for ~72 hours (short-term tests) and up to 28 days (long-term tests). The short-term-test samples were subsequently exposed to high-pH fluid (sodium hydroxide solution) under the same pressure and temperature conditions to investigate the gel breakdown when exposed to alkaline solutions. For homogeneous, continuous gel samples, the gel strength was characterized by performing a mechanical compaction (squeezing) test. The gels produced from high Si/Na ratio sodium silicate solution and moderate concentration acids (HCl and acetic acids) exhibited varying degrees of gel shrinkage (syneresis) and gel collapse. When mixed with high pH NaOH solution, the gels disintegrated and exhibited significant volume reduction. In contrast, metal silicates were stable and did not show visible changes when exposed to $NaOH_{aq}$. The experiments so far indicates that a combination of high-concentration sodium silicate (10 wt%) and acetic acid (4.6 wt%) produces a high-water-content silica gel that is stable under a high-temperature, closed (no-flow) environment. The objective of this work is to identify materials that can be used to seal unwanted fast-flow pathways in an EGS reservoir, with the potential of dissolving these plugs if needed.

1. INTRODUCTION

High permeability fractures connecting injection and production wells serve as fast flow paths that may function as undesired short circuits, leading to premature thermal breakthrough. This research investigates the possible use of hydrated silica gels, formed and stable under EGS-relevant conditions, to block the short circuits and can be removed later to recover the permeability either by dissolving or collapsing the produced materials. Sodium silicates and the gels produced from them have been employed extensively for shallow soil stabilization (e.g., Hurley and Thornburn, 1971) and for oil and gas and geothermal well stabilization (e.g., Liu and Ott, 2020). The use of silica gel as a flow diverter in EGS applications has been considered previously (e.g. Hunt et al., 2012). Because the targeted area of treatment by the gels is away from the injection well, a special consideration is required to control the location and timing of the gel diverter plug formation.

Our on-going project funded by US DOE-GTO (DE-EE0002498) aims to develop a technology for achieving this by delivering at least one component of the gel-forming chemicals within ten-to-hundreds-micron-size microcapsules with a polymer shell that can thermally degrade at EGS temperatures (Figure 1). We selected silicate-based flow diverters for its many advantages. These include (1) the ability to form fast-setting plugs at high temperatures, (2) the stability of the plug at the high temperature over extended periods, compared to thermally-degrading organic gels, (3) the possibility for the gel to dissolve or decompose easily when exposed to highly alkaline fluids, and (4) the environmentally friendly nature of silica gel. The use of microcapsules not only helps control the timing of reaction but also ensures hazardous chemicals, such as acids, can be safely handled and do not damage drilling equipment during injection.

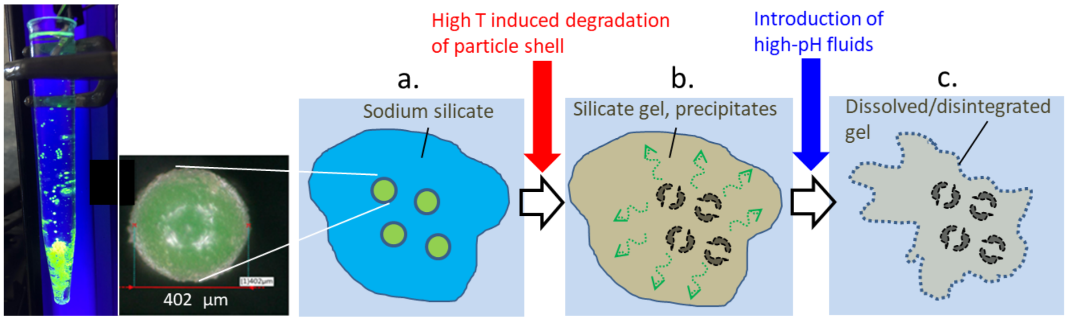

Figure 1: Concept of silicate gel and precipitate-based flow diverter plug formation in EGS reservoirs via encapsulated microparticles. Currently produced model particles are shown on the left. Thermal degradation of a polymer shell releases gelation/precipitation-inducing chemicals. The diverters are later removed by injection of high-pH fluid.

Sodium silicate (SS) solution starts to crosslink and form gel when its pH is reduced. This is believed to progress by producing increasing longer molecular chains (monomer, dimer, trimer etc.) by absorbing H^+ ions (e.g., An-Peng, 1963). Because this process produces additional OH^- ions in the solution, SS acts as a pH buffer. Acid and other chemicals are used to provide H^+. However, because the gelation proceeds rather slowly, if strong acids (e.g., HCl, H_2SO_4, HNO_3) are used, the pH of the acid before mixing and also the initial pH of the acid-SS mixture can be very low, causing safety concerns and potential corrosion of well casings. In contrast, weak acids (e.g., acetic acid, citric acid, formic acid) can keep the pH at an acceptable level, and by counteracting the SS's buffering effect, they provide the necessary amount of H^+. This also becomes important when the acid is delivered via microcapsules, because the total amount of the acid that can be delivered to the target location would be limited by the volume concentration of the particles in the injected fluid, making it necessary to use highly concentrated acid. When organic weak acids are used, however, their temperature stability under the EGS conditions can be an issue. In this research, we consider acetic acid, because it has been shown to be stable up to ~230°C for 72 hours (Li et al., 2017). At higher temperatures, acetic acid starts to decompose and produce CO_2 and CH_4.

The performance of hydrated silicate gel and metal silicate-based flow diverters under the EGS conditions is affected by several factors including their formation time, long-term stability, and dissolvability. The diverters need to form under realistic in-situ conditions such as achievable concentrations of SS and gel/precipitation activators (e.g., acids and metal cations, respectively) and reasonable reaction time. Once formed, the diverter needs to keep its integrity and shear strength. High-porosity gels can shrink spontaneously and lose the pore fluid over time, eventually leading to gel structure collapse ("syneresis"). The shear strength of the gel can also evolve over time, although the strength necessary for diverting the reservoir fluid flow away from the wells may not be as high as the near-well environment experiencing a steep pressure gradient. Lastly, silicate gels can dissolve rapidly at high temperatures if exposed to water out of equilibrium with silica, particularly at high pHs (e.g., Rose et al., 2007). The large surface area and weaker molecular bonds of gel can lead to even higher dissolution rate compared to low-porosity, crystalline and amorphous quartz. This aspect, however, also ensures that the silicate gel diverters "do no harm", i.e., the reservoir permeability naturally recovers if an unintended loss of permeability occurs, and also helps accelerated removal of the diverter via injection of high pH fluids if necessary.

Although silica gels and metal silicates have been used for geotechnical applications for nearly a century, their performance as a flow diverter under the EGS conditions still have not been well characterized. Our current preliminary study focused on the initial formation and the stability of acid-induced silicate gels and metal silicates in a closed (i.e., no-flow) aqueous environment under 200°C. In the following, laboratory experiments investigating both short (72 hours) and long (up to 1 month)-term behavior of the produced materials is presented.

2. EXPERIMENTAL SETUP

2.1 Materials

The aqueous sodium silicate (SS) solution used in this research was obtained from Cole Palmer (product#SS338-1), with a mass concentration of 38.3 wt%, and a SiO_2-to-Na_2O mass ratio of 3.21 (molar ratio 3.31) (based upon manufacturer-provided data on MSDS sheets). Using this ratio, the molecular formula can be expressed as $(Na_2O)_x(SiO_2)_y$ where x=0.5, y=1.66. For producing pH-induced silicate gels, we used both $HCl_{aq.}$ and acetic acid. For metal silicates involving polyvalent cations such as Ca^{2+} and Al^{3+}, we used $CaCl_2$ and $AlCl_3$, respectively.

2.2 Equipment

The primary equipment used in this research is a series of small, stainless-steel Parr reactor vessels. By design, these vessels accept a small Pyrex or stainless steel cup holding a test sample. Although we initially used these cups for the experiment, we identified several problems with this setup, including potential loss of fluid during a test, contamination of the sample by the residual materials on the pressure vessel wall, and transfer of liquid between the sample cup and the gap between the cup and the vessel wall. Therefore, to minimize these risks, we also used small, sealable internal cells made of corrosion-resistant grade-2 titanium. Six identical cells with screw-in tops with an o-ring seal were fabricated (Figure 2). High-temperature Viton o-rings rated for 230°C were used. The experiments presented in this paper demonstrated that the seals can contain water vapor at 200°C without any loss even over 1 month.

a. Sealable titanium (grade 2) mini cells

b. Parr reactor vessels

Figure 2: Equipment used for gel formation and stability tests. To minimize fluid loss and chemical contamination of the samples, sealable internal cells (a) were used in combination with small Parr reactor vessels (b). These vessels were heated in a convection oven at 200°C.

The mechanical response of the gels and precipitates to compression loading was examined using compaction test systems that drive a flat-bottom plunger into the test cell. During compaction, the pressurized material is squeezed through the annular gap between the plunger and the internal cell wall. The larger system (Figure 3a) involved a cylindrical stainless steel test cell with an inner diameter of 38.51 mm and a plunger with a diameter of 38.384 mm, resulting in a gap width of 63 µm. The compression was applied via an MTS system using a hydraulic ram, and the reaction force was measured using a strain-gauge load cell. A smaller system (Figure 3b) used the sealable titanium cell in Figure 2 with the inner diameter of 25.4 mm and the plunger diameter of 22.2 mm, yielding the gap width of 1.59 mm. For this system, the load was applied using a piezoelectric drive (NEXLINE N-216.2A, Polytech PI), which can apply precise displacement and displacement rates. The resulting force was measured using a strain-gage load cell (MLP-75, TransducerTechniques). The test system was controlled using a LabView^{TM} code, which was also used for data acquisition.

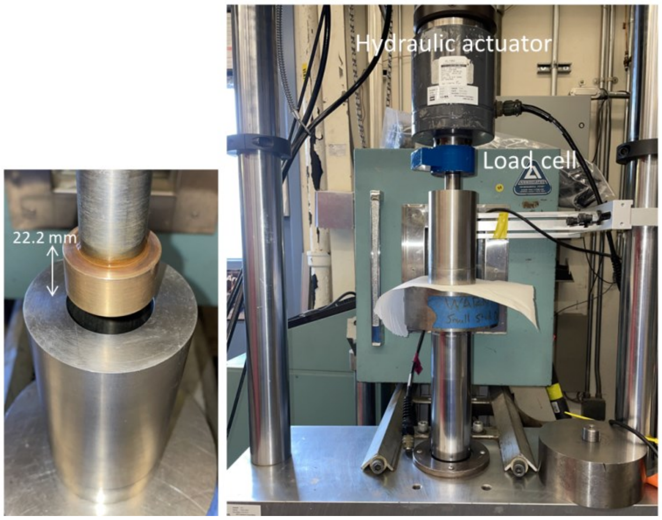

a. Larger, narrow-aperture (gap) compaction system

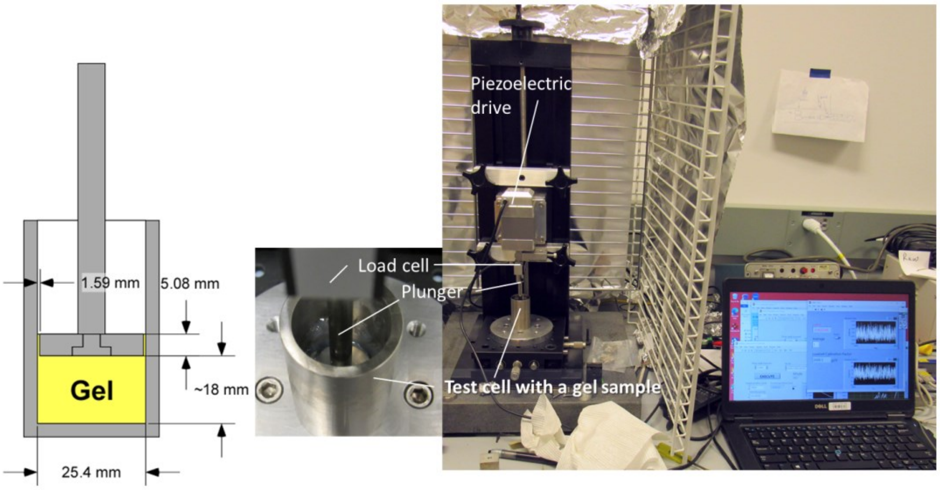

b. Smaller, wide-aperture (gap) compaction system

Figure 3: Laboratory systems used for compaction tests. Gels and precipitates were uniaxially compressed and squeezed between a gap between a vessel wall and a piston. A larger setup had a narrow gap width of 63 µm, and the smaller setup had 1.59 mm.

2.2 Test Procedures

2.2.1 Short-Term Tests (72 hours)

Short-term tests were conducted using 5 wt% SS (unless noted) and the activators shown in Table 1. The mixing of the components was done at room temperature. Once the chemical components were mixed homogeneously, the samples were heated at 90°C for 1 hour ("Initial formation test"). Subsequently the samples were introduced in Parr reactor vessels. Note that for these tests unsealed Pyrex and stainless steel sample containers were used to hold the samples in the reactor vessels. The vessels were then placed in a convection oven heated at 200°C for 72 hours, to examine the stability of the gels and the precipitates ("Stability test"). Because no attempt was made to control the pressure of the vessels during the experiment, we assume that the samples were under the vapor pressure of the liquid (for pure water, 1.55 MPa) contained in the samples.

Table 1: Gelation/precipitation activators used in the short-term tests

Activator	Concentration (wt%) when mixed with SS
$HCl_{aq.}$	0.00003, 0.003, 0.3, 1, 1.5, 2, 3
CH_3COOH	1, 2, 5
$CaCl_2$	0.1, 0.5, 1
$AlCl_3$	0.1, 0.5, 1

After the initial 72 hours, the samples were removed from the oven and the vessels, and the 0.1 M NaOHaq. (pH~13) was poured into the sample containers by approximately the same amount as the original sample volume. These samples were then reintroduced in the pressure vessels and heated again at 200°C for 72 hours ("Dissolution test").

After the initial heating at 90°C and the stability test and then the dissolution test at 200°C, the samples were examined visually and the pH of the free liquid on the samples was measured. Because of its destructive nature, the compression test described in Section 2.2 was also performed at each stage by using multiple samples with the same compositions, except for the acetic acid-activated samples after the dissolution test, which used already compressed samples from the preceding stability test.

2.2.2 Long-Term Tests (Up to 28 days)

We tested two combinations of SS and acetic acid concentrations for the resulting gel's long-term stability. One was Gel A: 5 wt% SS and 2 wt% acetic acid (this combination was also used previously in the short-term test), and the other was Gel B: 10 wt% SS and 4.6 wt% acetic acid. The concentration of acetic acid in the latter case was determined in such a way that the molar quantity of Na^+ was matched with the acetate ions (CH_3COOH^-), assuming the reaction

$$(\mathrm{Na_2O})_x(\mathrm{SiO_2})_y + 2x\mathrm{CH_3COOH} \rightarrow (\mathrm{SiO_2})_y + 2x\mathrm{CH_3COONa} + x\mathrm{H_2O}\cdot \qquad (1)$$

The gels were formed directly wthin the sealable titanium cells by mixing the inredients vigorously for 30 s using a glass rod at room temperature. Gelation initiated within ~20 minutes after mixing. For this test, the initial heating at 90˚C conducted for the short-term tests was not conducted. After 1 hour at room temperature, the samples were introduced into pressure vessels, then heated in a pre-heated convection oven at 200˚C. A batch of samples, each weighing 10 g, were prepared so that characterization tests including destructive loading tests can be conducted for samples with a range of heating durations. Using the sealable, leak-free cells, the synerisis behavior of the gels can be examined quantitatively. The bulk density and the volume fraction of the gels lost due to syneresis were determined gravimetrically. Also, the pH of the free fluid was measured using a pH meter.

3. RESULTS

3.1 Short-Term Tests (72 hours)

3.1.1 HCl gels

For HCl gels, gelation occurred only for acid concentration of 1 wt% and above. Although gelation occurred very quickly within 20 s for 1 wt% (pH~10), for higher concentrations, gelation did not happen even after the initial formation test at 90°C. Initial pH for the 3 wt% sample was ~0. Also, for 1.5 and 2 wt%, the gel was heterogeneous with solid particles settled at the bottom of the container. After the stability test, 1 wt% gel collapsed due to severe syneresis. In contrast, higher concentrations resulted in solid gels (Figure 4). The initial lack of gelation for the high concentration cases can be explained by the fact the gelation time increases for both high and low pHs (e.g., PQ Europe, 2004, page 7). Once gelation (polymerization) initiates, the pH of the mixture increases, accelerating further gelation.

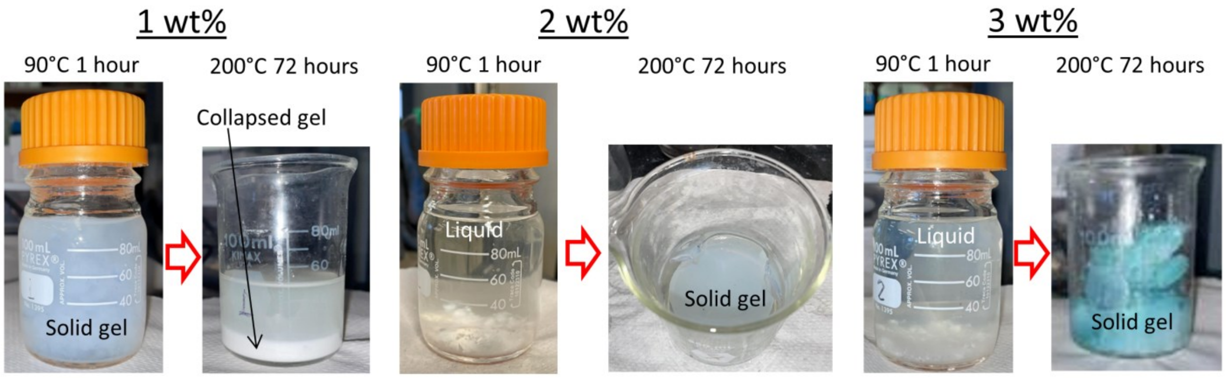

Figure 4: Examples of HCl-activated SS gels. 1 wt% gel formed immediately during the initial formation test (before heating), but the gel collapsed during the stability test at 200°C. Higher-concentration samples did not start to gel in 1 hour at 90°C, but formed solid gels during stability test. For 3 wt% gel, the acid reacted with the stainless steel vessel wall, resulting in contamination of the sample.

After the dissolution tests, 1.5 and 2 wt% gels completely disintegrated into particles and liquid at pH~10-11. In contrast, 3 wt% gel maintained its integrity. The pH of the mixture however was only ~7, indicating that neutralization by the remaining acid impeded the ability of $NaOH_{aq}$ to dissolve the gel. Additionally, HCl reacted with the stainless vessel wall, resulting in changes in the color of the fluid with the sample. More studies are needed on how the dissolved iron in the fluid directly impacted the gel dissolution.

A summary of the compaction tests is shown in Figure 5. All the results are for a loading rate of 0.1 mm/s. The responses can be categorized into two types based upon the roughness of the curves. Rough curves seem to indicate the response is due to the solid gel's visoplastic response involving tensile rupture and shear grinding. In contrast, smooth curves with shorter displacements indicate responses of high-viscosity liquid. The stress for the latter can also be very high, because this series of experiments was conducted using the test system in Figure 3a with a very narrow gap (t=63 µm) between the test cell and the loading piston. Both gel shrinkage (syneresis) and disintegration of solid gel can result in shifts of the solid curves to the right. Also note that the piston displacement is limited to <~25mm by the bottom of the container.

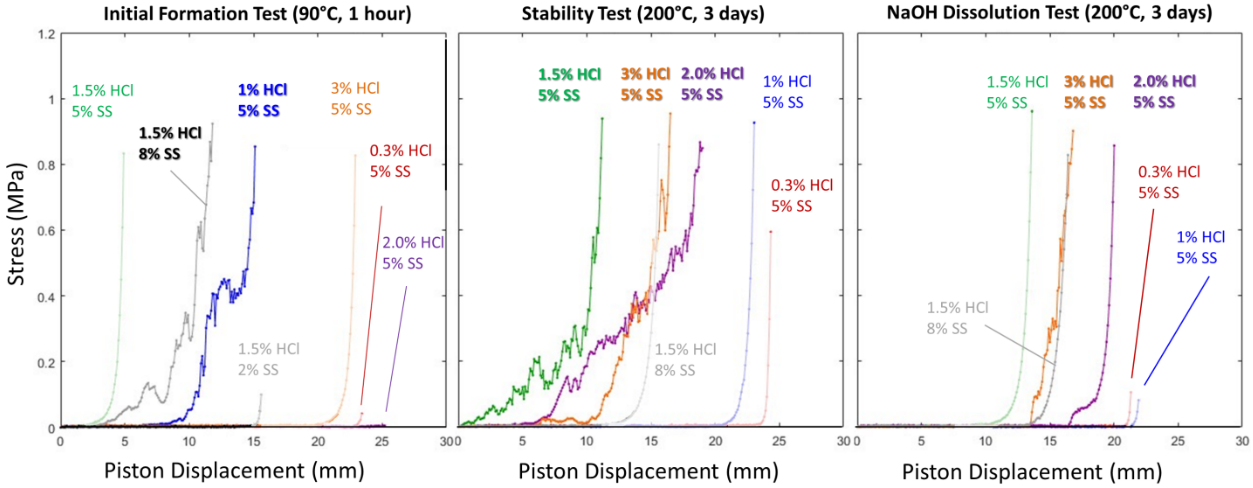

Figure 5: Stress-displacement relationships obtained for SS gels with a range of HCl and SS concentrations. Note that the only the curves with a rough profile indicate responses of solid gels. Because of the very narrow gap through which the sample is squeezed through, the smooth curves indicate fluids with a range of viscosity. A high viscosity results in high stress. Also note that once the piston is displaced for ~20 mm, it starts to press against the cell bottom. The loading rate was 0.1 mm/s.

3.1.2 Acetic acid gels

For acetic acid gels, three tested concentrations of the acid all resulted in quick gelation (Figure 6a). Both 2 wt% and 5 wt% gels formed in less than 5 minutes after mixing, and 1 wt% gel formed during the initial heating at 90°C. The pH values for the free liquid (produced by small syneresis) after 1 hour were 11 (1 wt%), 9.8 (2 wt%), and 3.3 (5wt%). After the stability test at 200°C for 72 hours, the samples turned opaque, and the pH of the free liquid changed to 11.7 (1 wt%), 9.8 (2 wt%), and 4.6 (5 wt%). Similar to the HCl case, 1 wt% gel collapsed to form hard precipitates. Although both 2 wt% and 5 wt% gels kept their integrity, a large amount of free liquid was produced. Particularly, 5 wt% gel developed visible tensile cracks in the sample (Figure 6b).

Next, the gels were mixed with high-pH (~13) NaOH solution and, again, heated at 200˚C for 72 hours. 2 wt% gel collapsed and/or disintegrated and formed hard precipitates (Figure 6c). 5 wt% acid gel appeared to maintained its integrity. Measured pH values were 11.7 (1 wt%), 11.3 (2 wt%), and 9.8 (5 wt%). It was not clear from this experiment if the disintegration of the 2 wt% gel was caused by the elevated pH or by continued syneresis.

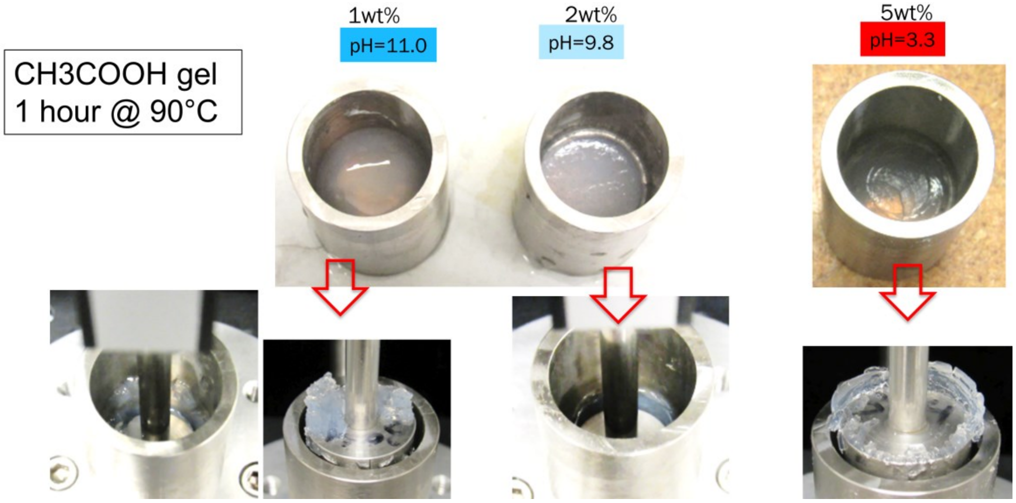

a. Initial gel formation

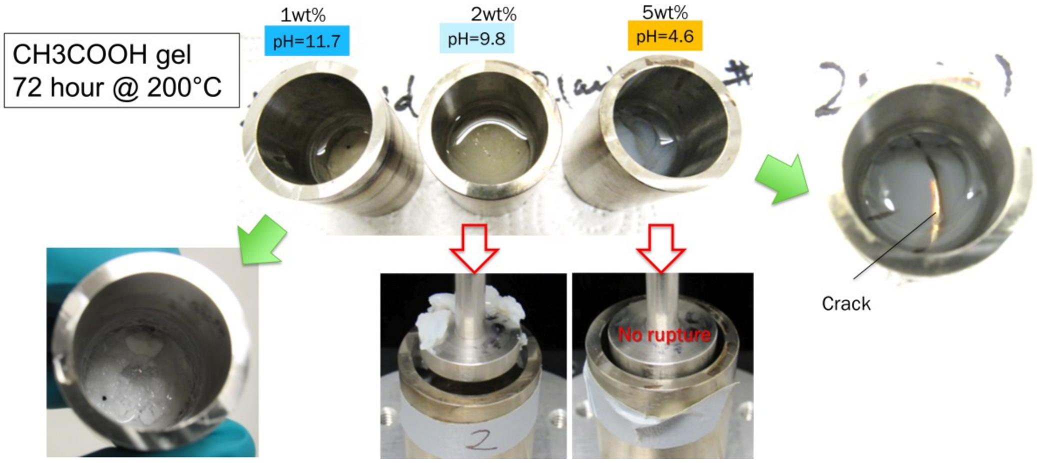

b. Stability test

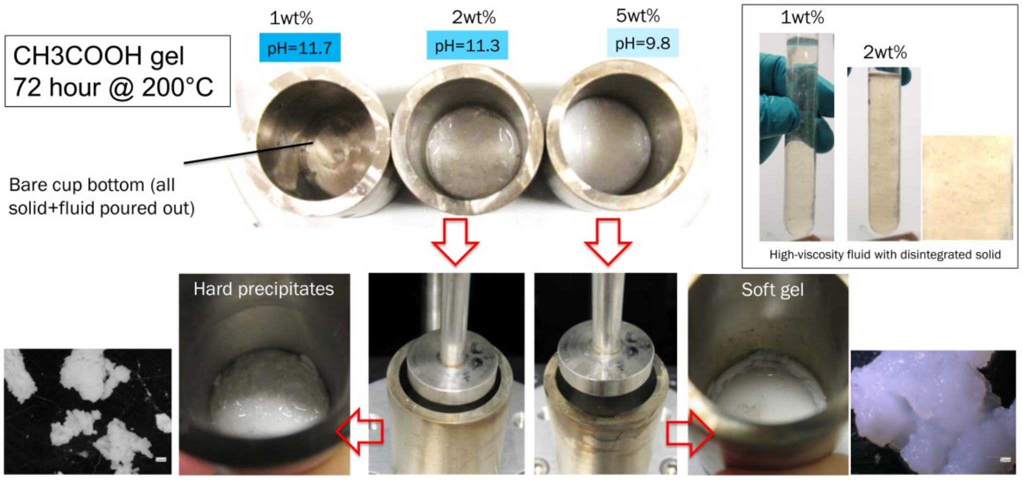

c. Dissolution test using $NaOH_{aq.}$

Figure 6: Acetic acid gel tests for three acid concentrations. Initially, all formed transparent-to-translucent solid gels. After the stability tests, 1 wt% gel collapsed, but 2 wt% and 5 wt% gels were stable, but with strong syneresis. Upon mixing with pH=13 $NaOH_{aq.}$, 2 wt% gel disintegrated, but 5 wt% gel maintained its integrity.

The compaction test results are shown in Figure 7 for the acetic acid-induced gels. All the results are for a loading rate of 0.1 mm/s, and the smaller test cell system shown in Figure 3b was used. Because of the wider gap (1.59 mm) compared to the HCl gel tests, the resulting stresses are smaller, and the rupture strength of the gels are better defined (indicated by horizontal arrows in the plot). Note that for this test, the initial position of the piston was at the top of the gel sample, regardless of the amount of shrinkage. Heating at 200°C significantly reduced the load-bearing capability of the gel. Additionally, the stress-displacement response did not show clearly defined rupture strength, showing only gradual increases in the stress. In the test after the dissolution test, the stress for 2 wt% sample increases abruptly, because the gel collapsed and the piston immediately started to compress the hard precipitates at the bottom of the test cell. Also, although the 5 wt% sample seemingly exhibits higher strength, this is because the dissolution test for this sample was conducted on the same sample that was used for the stability test and was already compacted once.

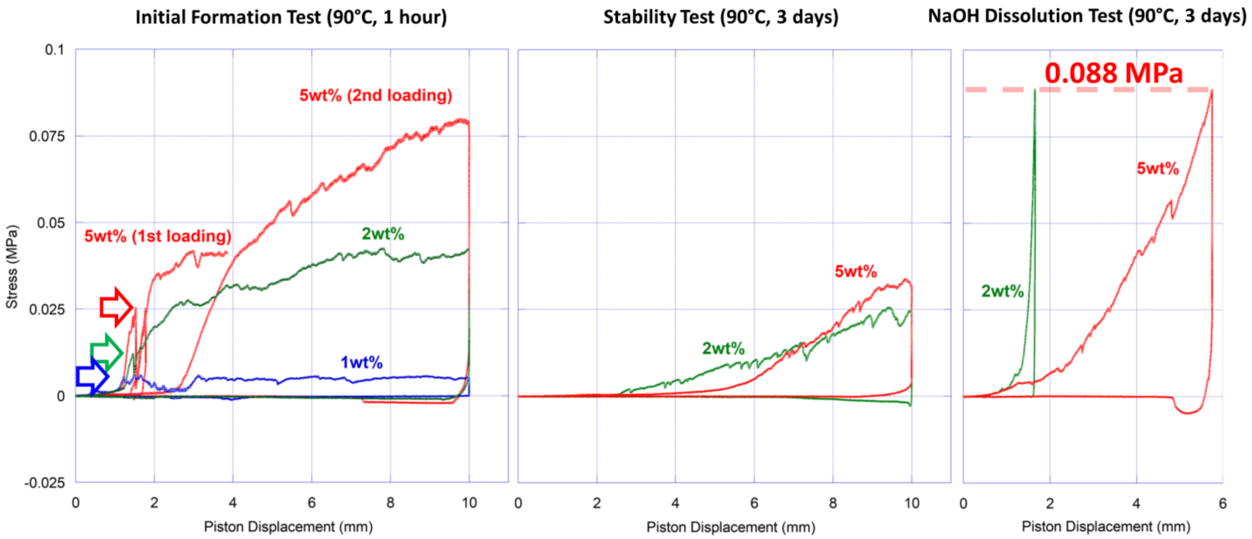

Figure 7: Stress-displacement relationships obtained for SS gels with different acetic acid concentrations. For these tests, clearly defined initial gel strengths (rupture strength) were measured (indicate by arrows). Note that loading was started at the top of the sample, with the maximum displacement of 10 mm and the stress of 0.088 MPa. Because of large shrinkage of the samples, the piston reached the bottom of the test cell for the 2 wt% sample.

3.1.3 Ca and Al silicate tests

Unlike acid-activated gels, Ca and Al salts resulted in almost immediate reaction with SS solution, producing fine, powder-like precipitates (flocs) separated from the liquid portion. There was no significant cohesion between the precipitates. For calcium-induced precipitates (calcium silicate [CS]), the initial pH after 1 hour of 90˚C heating was 11.1 (0.1 wt%), 11.0 (0.5 wt%), and 10.9 (1 wt%). For 0.5 wt% and 1 wt% samples, translucent and continuous gel also formed at the top of the samples. This transparent gel, however, disappeared after heating at 200˚C for 72 hours. The pH values slightly reduced to 10.3 (0.1 wt%), 10.9 (0.5 wt%), and 9.7 (1 wt%). As suspected, the introducing high-pH $NaOH_{aq.}$ had little impact on metal silicates (Figure 8).

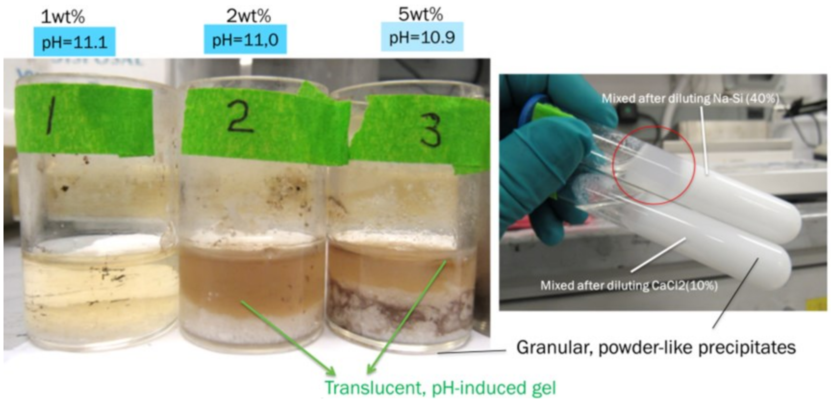

Figure 8: $CaCl_2$ induced metal silicates after 1 hour of heating at 90˚C. Upon mixing, all the samples immediately formed loose precipitates (flocs) with no cohesion.

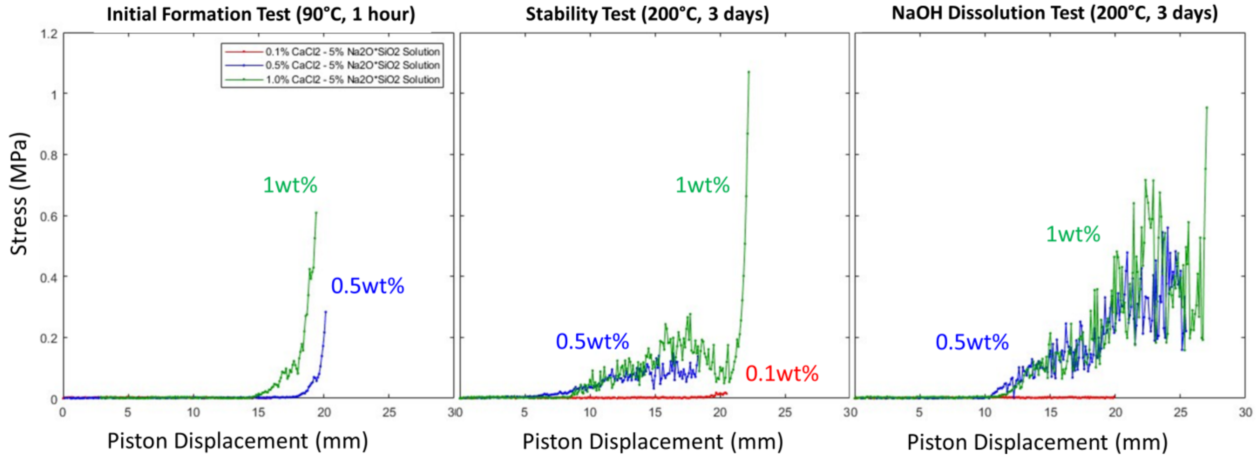

a. $CaCl_2$ tests

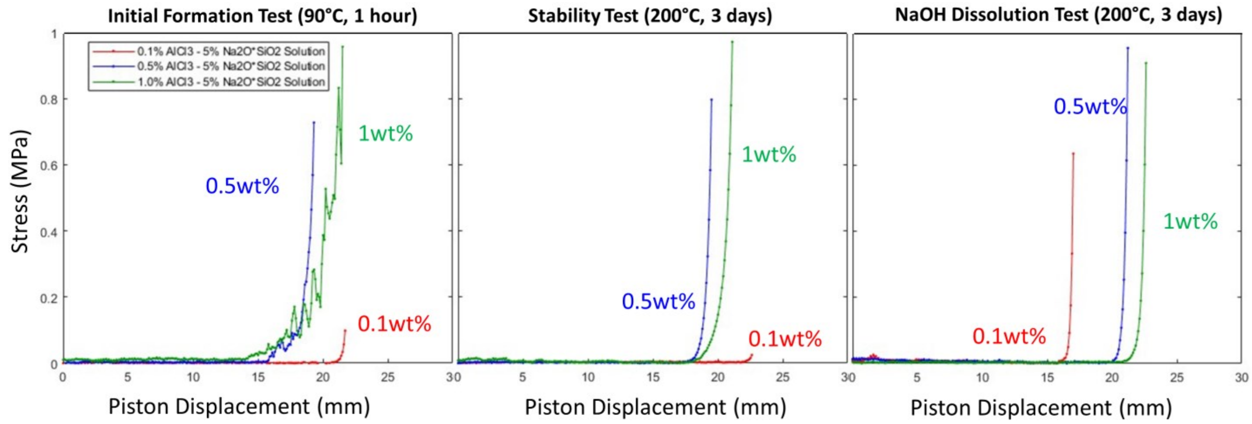

b. $AlCl_3$ tests

Figure 9: Calcium silicate (CS) and aluminum silicate (AS) compaction tests. Both form loose powder-like precipitates separated from liquid. CS is stable under 200˚C, and hardly affected by elevated pH. In contrast, the response of AS changed from that of solid-fluid mixture to viscous fluid. However, the solid particles were visibly present in the mixture (the apparent stress increases are caused by the piston hitting the bottom of the test cell).

The compaction test results are shown in Figure 9a for the calcium silicate (CS) and in Figure 9b for aluminum silicate (AS). The tests were conducted using the setup in Figure 3a. For CS, because the precipitates form a loose layer (flocs) at the bottom of the test cell, the stress response is mainly due to the compaction of this layer. The viscosity of the fluid is very low and contributes little to the measured stress. As mentioned earlier, the sudden increase of stress is due to the piston starting to press against the cell bottom (note that the initial location of the piston in the cell was not well controlled). The larger stresses measured for the tests after introducing $NaOH_{aq}$. may be attributed to the precipitation of NaCl in the cell. The initial responses of 0.5 wt% and 1 wt% AS are very similar to CS. However, heating seemed to change the nature of the precipitated particles, and the force-displacement responses showed smooth, gradual changes similar to viscous liquid. However, solid particles were still visible in the mixture. The pressure response after the stability test and dissolution test are from the piston-cell bottom interactions.

3.2 Long-Term Stability Tests (Up to 1 month)

Long-term tests were conducted only for acetic acid activated gels (see Figure 10). Gel A with lower concentration of SS and acetic acid initial exhibited slow syneresis. However, after 5 days, the gel suddenly shrunk and collapsed, losing near 90% of the original volume. In contrast, after similar initial behavior, Gel B was generally stable even after 28 days. (Note that there is one anomarous data point at day 14, showing rather strong syneresis, but considering the following two longer-duration data points, we suspect this was caused by an unknown experimental error.) pH of the fluid for Gel A initially increases, possibly due to continuing progress of gelation which produces OH^- ions. After about 1 week, however, pH started to drop towards the neutral value. Note that the pH was measured after the fluid and the gel sample was cooled to room temperature. In contrast, although there was a slight initial increase, pH for Gel B showed only small changes at slightly acidic pH=6, which gradually dropped to pH~5.5. The reason for the decreasing pH for longer-duration tests is not known, but we suspect that it may be attributed to the CO_2 produced by slow decomposition of acetate (CH_3COO^-) and/or to HF produced from the reaction between steam and the Viton. Microscope images of Gel A and Gel B at Day 10 clearly indicates the morphological differences between the near-totally collapsed gel and stable gel (Figure 11). The collapsed gel shows uniformly sized

(~5 µm) hard spherical paricles of precipitated silica. In contrast, the stable gel stays plastic, and does not show development of such microstructure.

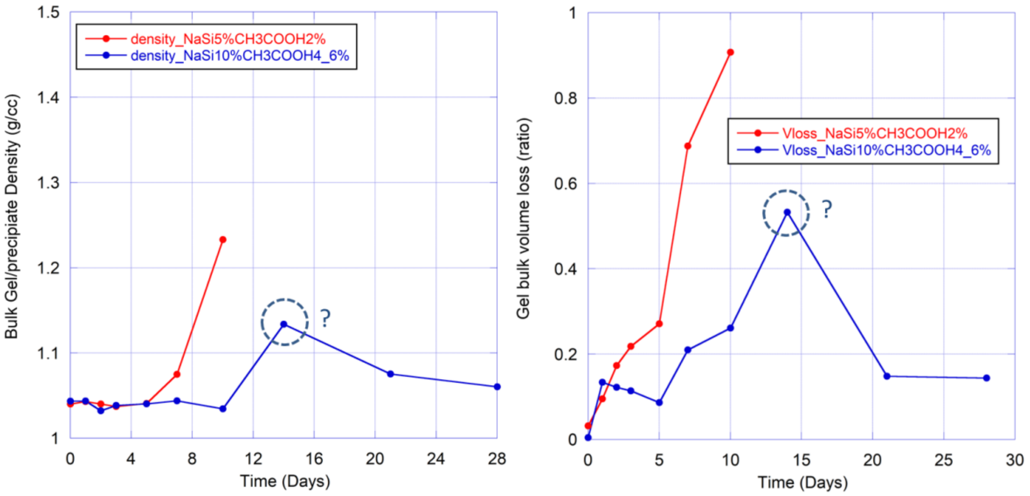

a. Gel bulk density

b. Syneresis (volume loss fraction)

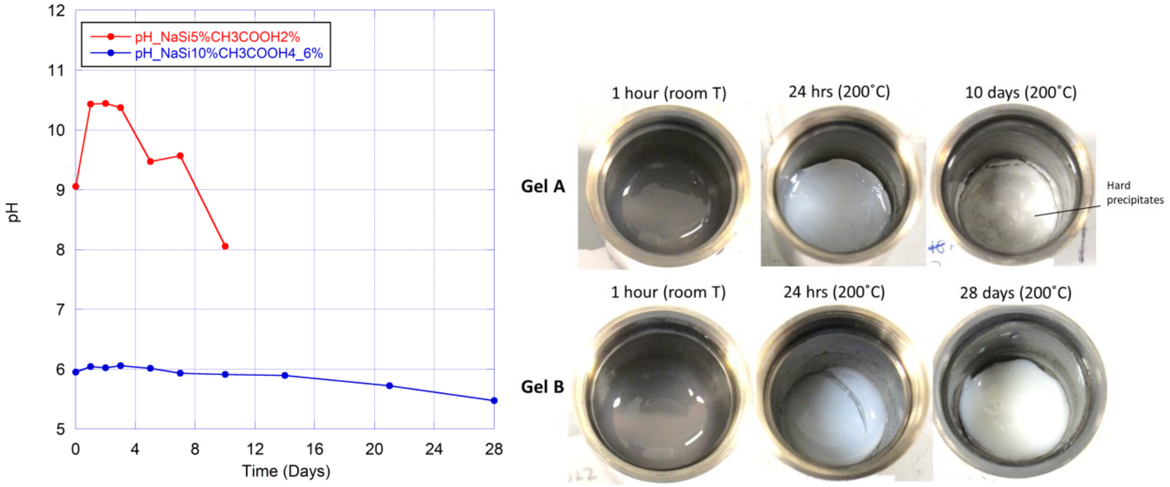

c. Free liquid pH

d. Photo images of the gels

Figure 10: Comparison of two series of tests on acetic-acid-induced silicate gels. Gel A: 5 wt% SS + 2 wt% acetic acid, Gel B: 10 wt% SS + 4.6 wt% acetic acid. Gel B exhibits much less syneresis, even after one month. The cause of the anomalous data for Day 14 is not known.

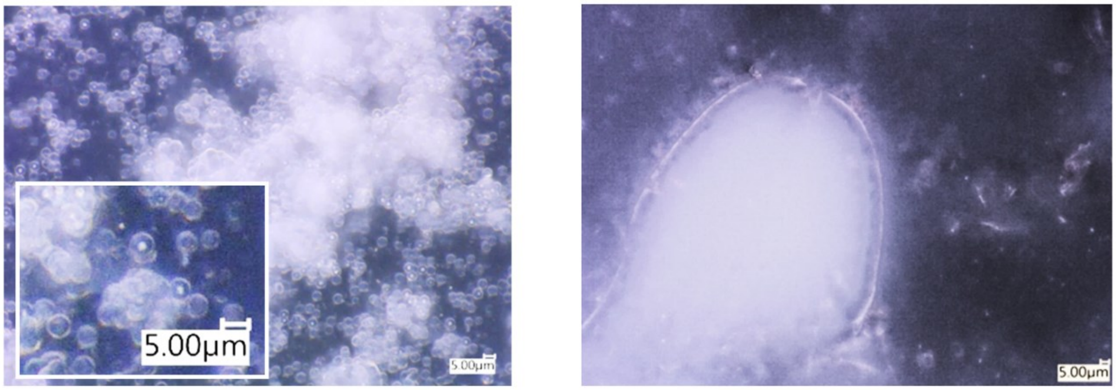

a. 5wt% SS, 2wt% acetic acid gel

b. 10wt% SS, 4.6wt% acetic acid gel

Figure 11: Comparison of samples after 10 days of heating at 200˚C. Nearly totally collapsed low-concentration gel (a) formed hard microspheres of uniform size (diameter~5 µm). In contrast, the higher-concentration gel stayed continuous and plastic, without such precipitation. The samples shown here were squeezed between two microscope slides.

Finally, the results of compaction tests are presented in Figure 12, for a constant displacement rate of 0.1 mm/s. For these plots, the starting point (-5 mm) of the displacement was fixed at ~2 mm above the surface of the original, non-heated gel in the test cell. The red arrows indicate the strength of each gel when the initial rupture occurred. As seen in the short-term test, heating at 200˚C for only 1 day causes significant drops in the load-bearing capability of the gels. We do not think these changes can be explained by the syneresis alone, because the reductions of the gel volume are only ~10%, at least initially. Instead, we speculate that this is caused by increase in the flow permeability of the bulk gel matrix, which causes accelerated volumetric compaction of the gels. This may be supported by several observations including (1) increased opaqueness of the gels, which indicates coarsening of silica particles and the accompanying permeability increase, (2) general lack of extruded materials after the compaction tests on heated samples, and (3) smoother load-displacement curves. Both (2) and (3) indicate that the compaction was caused by poro-(visco) plastic compaction and release of low-viscosity liquid, rather than the shear flow of broken gel matrix squeezed through the cell gap.

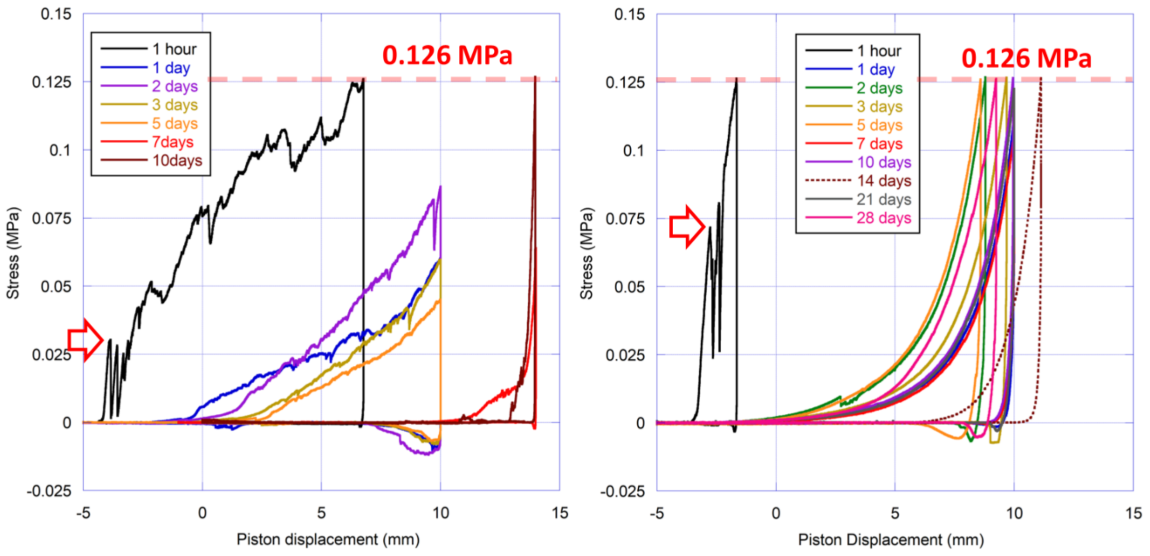

a. 5wt% SS, 2wt% acetic acid gel (Gel A)

b. 10wt% SS, 4.6wt% acetic acid gel (Gel B)

Figure 12: Stress-displacement relationships for SS gels with two different acetic acid concentrations and heating durations. Only pre-heating samples exhibit well-defined gel rupture strength (shown in red arrows). In these plots, the displacements are all referenced to the test cell bottom located at 14 mm. Note that the maximum loading limit is 0.126 MPa, and the displacement is 10 mm. For samples exhibiting severe syneresis, the initial piston location was offset to increase the maximum displacement range. Compared to Gel A, Gel B's mechanical response is generally unchanged, indicating the stability of the gel at 200°C.

4. CONCLUSIONS

We observed sodium-silicate gels produced from HCl and acetic acid exhibited a varying degree of stability against gel syneresis under 200°C. With acetic acid, for 5 wt% sodium silicate concentration, higher concentrations of the acetic acid (2 and 5 wt%) resulted in stable gels. However, 2 wt% gel exhibited complete collapse after 7 days. For higher, 10 wt% sodium silicate and 4.6 wt% acetic acid, the gel was stable up to 28 days with only small syneresis. Mechanical tests indicated that compressed gels undergo large compaction with accompanying loss of pore fluid and increases in strength. Although both syneresis and dynamic compaction of the gels are undesirable for reducing fracture permeability, the shrunk gels may still provide sufficient permeability reduction of a high-permeability fracture. This is because naturally shrinking gels tend to collapse and clog constricting points and pore throats of flow pathways (Bryant et al., 1996), and also, the compaction of the gel by the differential flow pressure can create hardened, low-permeability plugs at these locations (Figure 13).

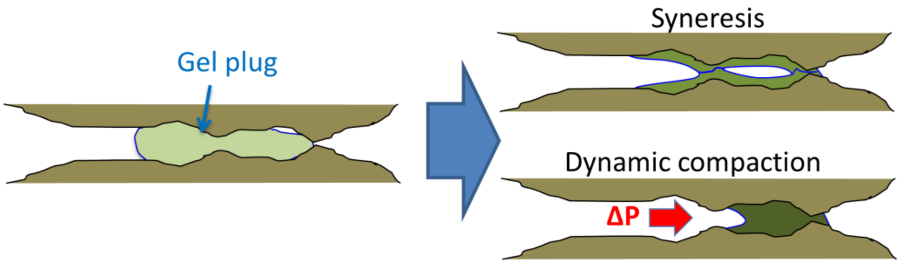

Figure 13: Possible scenarios for gel-plugged permeability changes in a fracture with flow constrictions.

The experiments so far have been conducted within a closed container under static, no-flow conditions. Under realistic EGS reservoir conditions, there will be exchange between the gel plugs, the adjacent pore fluid, and the surrounding environment, which will accelerate the dissolution of the silica gel plug. Although this cannot be prevented completely, the rate of dissolution may be reduced by taking measures such as (1) increasing the density of the gel, (2) co-injecting (e.g., calcium silicate) with the acid-induced gels. We will examine these possibilities by continuing the experiments in the current project.

ACKNOWLEDGMENTS

This work is supported by the U.S. Department of Energy, Office of Energy Efficiency and Renewable Energy (EERE), Office of Technology Development, Geothermal Technologies Office, under Award Number DE-AC02–05CH11231 with LBNL and contract DE-NA0003525 with SNL. Sandia National Laboratories is a multi-mission laboratory managed and operated by National Technology & Engineering Solutions of Sandia, LLC, a wholly owned subsidiary of Honeywell International Inc., for the U.S. Department of Energy's National Nuclear Security Administration. This paper describes objective technical results and analysis. Any subjective views or opinions that might be expressed in the paper do not necessarily represent the views of the U.S. Department of Energy or the United States Government. The authors would like to thank Drs. John Tuttle and Ron Tate (Sinclair Well Products) for valuable advice and suggestions. SAND2023-11645C.

REFERENCES

An-Peng, T.: A theory for polymerization of silica acid. Sci. Sin, 9(13111320), (1963), 15.

Bryant, S.L., Rabaioli, M.R., and Lockhart, T P.: Influence of syneresis on permeability reduction by polymer gels. SPE Production & Facilities, 11(04), (1996), 209-215.

Hamouda, A.A., and Akhlaghi Amiri, H.A.: Factors affecting alkaline sodium silicate gelation for in-depth reservoir profile modification. Energies, 7(2), (2014), 568-590.

Hunt, J.D., Ezzedine, S.M., Bourcier, W., Roberts, S., and Roberts, J.: Silica gel behavior under different EGS chemical and thermal conditions: an experimental study. Proceedings, Thirty-Seventh Workshop on Geothermal Reservoir Engineering, Stanford University, Stanford, California, (2012).

Hurley, C.H., and Thornburn, T.H.: Sodium silicate stabilization of soils: A review of the literature. Soil Mechanics Laboratory, Department of Civil Engineering, Engineering Experiment Station, University of Illinois, (1971).

Li, Y., Zhou, S., Li, J., Ma, Y., Chen, K., Wu, Y., and Zhang, Y.: Experimental study of the decomposition of acetic acid under conditions relevant to deep reservoirs. Applied Geochemistry, 84, (2017), 306-313.

Liu, S., and Ott, W.K.: Sodium silicate applications in oil, gas & geothermal well operations. Journal of Petroleum Science and Engineering, 195, (2020), 107693.

PQ Europe: Sodium and Potassium Silicates—Versatile Compounds for Your Applications, product brochure, (2004).

Rose, P., Xu, T., Kovac, K., Mella, M., and Pruess, K.: Chemical stimulation in near-wellbore geothermal formations: silica dissolution in the presence of calcite at high temperature and high pH. In Proceedings, Thirty-second Workshop on Geothermal Reservoir Engineering, Stanford University, Stanford, California, (2007).